Development 139, 929-939 (2012) doi:10.1242/dev.076794


# Bimodal control of Hoxd gene transcription in the spinal cord defines two regulatory subclusters

**Patrick Tschopp[1,*], Alix J. Christen[1,2] and Denis Duboule[1,2,‡]**


## SUMMARY

The importance of Hox genes in the specification of neuronal fates in the spinal cord has long been recognized. However, the transcriptional controls underlying their collinear expression domains remain largely unknown. Here we show in mice that the correspondence between the physical order of Hoxd genes and their rostral expression boundaries, although respecting spatial collinearity, does not display a fully progressive distribution. Instead, two major anteroposterior boundaries are detected, coinciding with the functional subdivision of the spinal cord. Tiling array analyses reveal two distinct blocks of transcription, regulated independently from one another, that define the observed expression boundaries. Targeted deletions in vivo that remove the genomic fragments separating the two blocks induce ectopic expression of posterior genes. We further evaluate the independent regulatory potential and transcription profile of each gene locus by a tiling array approach using a contiguous series of transgenes combined with locus-specific deletions. Our work uncovers a bimodal type of *HoxD* spatial collinearity in the developing spinal cord that relies on two separate 'enhancer mini-hubs' to ensure correct Hoxd gene expression levels while maintaining their appropriate anteroposterior boundaries.


**KEY WORDS: Hox genes, Collinearity, Transcriptional regulation, Mouse genetics**

## INTRODUCTION

Correct innervation of peripheral muscles by spinal cord motor neurons is a pre-requisite to initiate and coordinate body movements in all vertebrate species (Landmesser, 1978). In higher vertebrates, motor neurons are organized in different columns, such as the median motor column (MMC), the hypaxial motor column (HMC), the pre-ganglionic column (PGC) and the lateral motor column (LMC) (see Fig. 1A). It is believed that, in an ancestral system, an MMC-like column may have controlled an active swimming behaviour, as seen nowadays in jawless vertebrates, that essentially relies upon the undulating activation of the axial musculature all along the anterior to posterior (AP) axis (Fetcho, 1992). The appearance of a specialized column of motor neurons at the hindbrain-spinal cord boundary of ray-finned fishes may have set the ancestral stage for appendage innervation, the pectoral fin in this particular case (Ma et al., 2010). Subsequently, these columns and associated neurons functionally diversified and shifted to more caudal positions to meet the increased neuronal complexity required for controlling the musculature of tetrapod limbs (Landmesser, 2001; Ma et al., 2010). Neurons connecting to this complex muscular system are found in two major columns, the LMCs, which form two plexii at the brachial and lumbar levels. Within these columns, a stereotypic organization into discrete pools of motor neurons reflects their axonal trajectories, as well as their patterns of target innervation (Hollyday, 1980; Gutman et al., 1993).

National Research Centre 'Frontiers in Genetics' at [1]Department of Genetics and Evolution, University of Geneva, Sciences III, Quai Ernest-Ansermet 30, 1211 Geneva 4, Switzerland and [2]School of Life Sciences, Federal Institute of Technology EPFL, 1015 Lausanne, Switzerland.

*Present address: Department of Genetics, Harvard Medical School, 77 Avenue Louis Pasteur, Boston MA 02115, USA
‡Author for correspondence (denis.duboule@epfl.ch)

**Accepted 21 December 2011**

Transcription factors of the Hox gene family play essential roles in assigning motor neurons both their columnar fates and pools affiliations, along the AP axis (see Fig. 1A) (Dasen and Jessell, 2009). In mammals, 39 Hox genes are distributed into four distinct genomic clusters (*HoxA* to *HoxD*) and members of paralogy groups *Hox6* and *Hox10* have been functionally associated with the brachial and lumbar LMCs, respectively (Wahba et al., 2001; Dasen et al., 2003). By contrast, *Hox9* genes seem to determine PGC fates at thoracic levels (Jung et al., 2010). Within these columns, discrete patterns of different Hox proteins are thought to further define the subdivisions into the various motor neuron pools (Dasen et al., 2005).

The mechanisms leading to the required differential expression patterns of these genes along the rostral to caudal axis of the central nervous system (CNS) are less clear. Some of the upstream activating factors have been identified (Liu et al., 2001; Bel-Vialar et al., 2002; Nordstrom et al., 2006), yet whichever signal controls these genes, it will have to be interpreted in the context of their genomic clustering and translated into a collinear response along the AP axis, as an integral part of their transcriptional regulation (Kmita and Duboule, 2003). The mechanisms underlying this spatial collinearity in the CNS have long been studied in a transgenic context (e.g. Sharpe et al., 1998), yet they only recently started to be addressed using experimental approaches whereby a gene cluster was modified at the endogenous locus (Tarchini et al., 2005; Tschopp et al., 2009).

We set out to test and define which part of the global transcriptional outcome of the *HoxD* gene cluster in the developing spinal cord was due either to gene-specific features, or to regulatory modalities shared between various genes and thus linked to the genomic clustering of this gene family in vertebrates. To this end, we used tiling array-based transcriptome analyses to systematically assess the transcription of the *HoxD* gene cluster on a series of deletions stocks as well as in mice carrying contiguous Hoxd transgenes combined with the genomic deletions of the exact same loci. We report the presence of two major anterior boundaries,

which define independent blocks of transcriptional regulation, associated with the future plexii. Within each block, a delicate balance of promoter competition and sharing of 'enhancer mini-hubs' fine-tunes the correct establishment of spatial collinear Hox domains in the developing spinal cord.

## MATERIALS AND METHODS

### Mouse strains

Deletion alleles were produced in vivo using targeted meiotic recombination (TAMERE) (Herault et al., 1998b) and have been described elsewhere: Del(4-9) (Tschopp et al., 2009); Del(4-11) (Zacchetti et al., 2007); Del(9), Del(10), Del(i-9), Del(8-13)XII, Del(10) (Tarchini et al., 2005); Del(i), Del(8) (Tarchini and Duboule, 2006); Del(11) (Kmita et al., 2002). The novel Del(1-i) and Del(1-4) alleles (generously provided by B. Mascrez, University of Geneva) were generated using TAMERE with parental alleles Del(1-13)*d11*lac and L7 or L8, respectively, the latter strains carrying a single *loxP* site next to *Hoxd8* or *Hoxd4* (Tarchini et al., 2005). A novel *loxP* site 6kb telomeric to *Hoxd1* (tel1; L. Thévenet, F. Gonzalez and D.D., unpublished) was used to generate Del(tel1-13)*d11*lac. Timed matings were carried out using animals heterozygous for the respective alleles. Noon on the day of the vaginal plug was considered as day 0.5 of gestation (E0.5).

### Tiling array analysis

Custom-made oligonucleotide tiling arrays spanning a 2 Mb large region centred on the murine *HoxD* cluster were designed and manufactured by Affymetrix (see Soshnikova and Duboule, 2009). Embryos were dissected at E12.5 and stored in RNAlater (Qiagen) at –20°C until genotyping procedures were finished. Subsequently, spinal cords of positive embryos were dissected out and subdivided into three anatomically defined pieces along the AP axis: +2/–2 dorsal root ganglia (DRG) of the forelimb (brachial), +3/–2 DRG of the hind limb (lumbosacral) and the intervening fragment (thoracic). For each RNA extraction, spinal cords of two embryos were pooled, and total RNA was extracted using RNeasy Micro kit (Qiagen). Two micrograms of total RNA was used as starting material for rRNA depletion using the RiboMinus Human/Mouse Transcriptome Isolation kit (Invitrogen). RNA was subsequently reverse transcribed using random hexamers with a T7-promoter for one round of in vitro amplification of cDNA following the GeneChip Whole Transcript Amplified Double-Stranded Target Assay kit (Affymetrix). The resulting cDNA was fragmented and labelled using the GeneChip WT Double-Stranded DNA Terminal Labeling kit (Affymetrix) and hybridized onto our custom-made oligonucleotide tiling arrays. Genomic DNA used for normalization was fragmented with DNase I digestion. Arrays were hybridized, processed and scanned according to manufacturer's instructions (Affymetrix). Array data were normalized within cDNA/genomic DNA replicates using TAS software and scaled to medial feature intensity of 10 (Affymetrix, www.affymetrix.com). A sliding window of 80 bp was used to generate a data set consisting of all (PM-MM) pairs mapping within it. The averaged ratios were plotted along the genomic DNA sequence using Integrated Genome Browser (IGB) software (Affymetrix, www.affymetrix.com).

### In situ hybridization

Whole-mount in situ hybridization (WISH) and in situ hybridization (ISH) on slides were performed according to standard protocols. DIG-labelled probes for in situ hybridizations were produced by in vitro transcription (Promega) and detection was carried out using an alkaline phosphatase-conjugated anti-digoxigenin antibody (Roche). Probe templates were either as described elsewhere, or newly PCR-cloned from embryonic cDNA pools (the first and last ten nucleotides are given for orientation): *Hoxd3* (Condie and Capecchi, 1993), *Hoxd4* (Featherstone et al., 1988), *Hoxd8* (Izpisua-Belmonte et al., 1990), *Hoxd9* (Zappavigna et al., 1991), *Hoxd10* and *Hoxd11* (Gerard et al., 1996), *Hoxd12* (Izpisua-Belmonte et al., 1991), *HoxD-ig1* (CCAACCAGCT–ATGTCTGGAT), *HoxD-ig2* (GACCTA-TTTG–CTAGGCTCAA), *HoxD-ig3* (GGCATCTCTG–ATGTCTGGAT) *HoxD-ig4* (CCTAGGCATG–CTTGGTTCCT), *HoxD-ig5* (ATCTCT-GCTG–ATGATGAGGG), *HoxD-ig6* (CAAGGAATGA–TGGTGATG-GG). For WISH, embryos were dissected in PBS and fixed from 4 hours to overnight in 4% paraformaldehyde (PFA), washed in PBS, dehydrated and stored in 100% methanol at –20°C. Both mutant and control embryos were processed in the same well to maintain identical conditions throughout the WISH procedure and spinal cords were dissected out and flat-mounted. Images were globally processed for colour balance and brightness using Adobe Photoshop. For ISH, embryos were fixed for 90 to 120 minutes in 4% PFA in 0.1 M PBS at 4°C, washed extensively in PBS and cryoprotected in 30% sucrose, before embedding in OCT TissueTek compound. Cryoblocks containing mutant and representative wild-type control animals were fixed side by side and sectioned together, to guarantee identical hybridization conditions on the slide.

### TgN-*lac-loxP* series

For the generation of the *lacZ* transgene series spanning the *HoxD* clusters, genomic fragments corresponding to each *loxP-loxP* interval inside the complex were isolated and a *lacZ* cDNA was inserted in frame with the respective coding sequence of each Hoxd gene (see Fig. 4A and supplementary material Fig. S3). Fragment isolation was done with long-range PCRs (*Expand Long Template PCR System*, Roche) on purified genomic or bacterial artificial chromosome (BAC) DNA, using two pairs of oligos to generate a 5′ and 3′ fragment. In between, a unique restriction site was introduced to enter the *lacZ* cDNA with conventional cloning techniques. Moreover, a single *loxP* site was added to the distal primer of either 5′ or 3′ fragment, to singularize potential tandem copy arrays in vivo using Cre-deleter strains. Alternatively, *lacZ* cDNA was introduced by ET recombination into the mouse BAC 'RPCI23-400H17', leaving behind a single flippase recombination target (FRT) site after the removal of the selection cassette to be used for transgene singularization using an *Flp*-deleter strain (Yu et al., 2000). The resulting *lacZ*-tagged Hoxd genes were retrieved from the BAC by gap repair, using modified pBSK or pBR322 vectors containing homology arms derived from PCR products. For TgN*Hoxd9*lac and TgN*Hoxd11*lac transgenes previously generated in the lab were trimmed to match the cluster-internal *loxP-loxP* intervals and were modified with *loxP* or *FRT* sites to meet the requirements for singularization outlined above (Renucci et al., 1992; Gerard et al., 1993). Schematic overviews of the resulting plasmids are depicted in supplementary material Fig. S3. Final constructs were released from their respective backbone plasmids by restriction digest, gel-separated and dialysis-purified before pro-nuclear injection. At least two stable lines were established per transgenic construct and were crossed to either Cre- or *Flp*-deleter strains. Embryos were assessed for the regulatory potential of the respective constructs using whole mount detection of β-gal reporter activity (Zakany et al., 1988). For some constructs showing unexpected expression patterns, additional F0 embryos were stained for confirmation of the observed results if only two stable lines had been established.

### Immunohistochemistry

For immunohistochemistry (IHC), embryos were fixed for 90 minutes at 4°C in 4% PFA in PB and cutting was performed as for ISH (see above). IHC was performed following standard protocols. Primary antibodies were used at the following dilutions: goat anti-*Hoxd10* (1:500, Santa Cruz); rabbit anti-*FoxP1* (1:64,000, kind gift of Dr Jeremy Dasen, NYU School of Medicine). Secondary antibodies were donkey anti-rabbit Alexa Fluor 488 (1:1000, Invitrogen), biotin-conjugated donkey anti-goat followed by peroxidase-conjugated streptavidin (1:300, all Jackson ImmunoResearch) using for detection the Perkin Elmer TSA-Cy3 Kit. *FoxP1* quantification was done using biological triplicates. Six individual sections per replicate spanning the brachial plexus were stained for *FoxP1* and positive nuclei were counted. Excluding the highest and lowest values of these series, the values of the remaining four sections were averaged and counted as one replicate.

## RESULTS

We assessed the transcriptional status of the *HoxD* complex in the developing spinal cord by using custom-made tiling arrays covering a two megabase large DNA interval centred on the gene

cluster. We dissected out spinal cords at E12.5 and subdivided the cord into three anatomically defined fragments (see Materials and methods): firstly, an anterior piece containing the brachial plexus, which innervates the forelimbs; secondly, a posterior piece including the lumbosacral plexus that innervates the hind limbs; and, finally, the piece linking the two former fragments, referred to as the 'thoracic region' (Fig. 1A,B). RNA was extracted and processed for the three pieces at the same time and in the same conditions (Fig. 1B).

At brachial levels, only *Hoxd3* to *Hoxd8* were transcribed at detectable levels, with *Hoxd1* being silent at this stage (Fig. 1C). In addition to coding sequences, large stretches of intra- and intergenic DNA around *Hoxd3* and *Hoxd4* were also transcribed, starting from an alternative promoter of *Hoxd3* located in the *Hoxd4*/*Hoxd8* intergenic region (subsequently termed region 'i'). However, the intronic regions separating the coding exons of *Hoxd3* and *Hoxd4* were largely devoid of any transcripts (Fig. 1C). In the thoracic sample, no major changes were observed in the anterior transcription profile, whereas exon 2 of *Hoxd9* was now transcribed at a clearly detectable level. At lumbosacral levels, all genes from *Hoxd3* to *Hoxd11* were expressed at high levels, with some trace amounts of transcription detectable in more posterior parts of the cluster (Fig. 1E and supplementary material Fig. S1A-C). Here again, high amounts of intergenic transcription were scored, now also for the posterior part of the cluster (Fig. 1E), whereas throughout the complex we detected only minor amounts of transcripts originating from the 'non-Hox' DNA strand (supplementary material Fig. S1E,F).

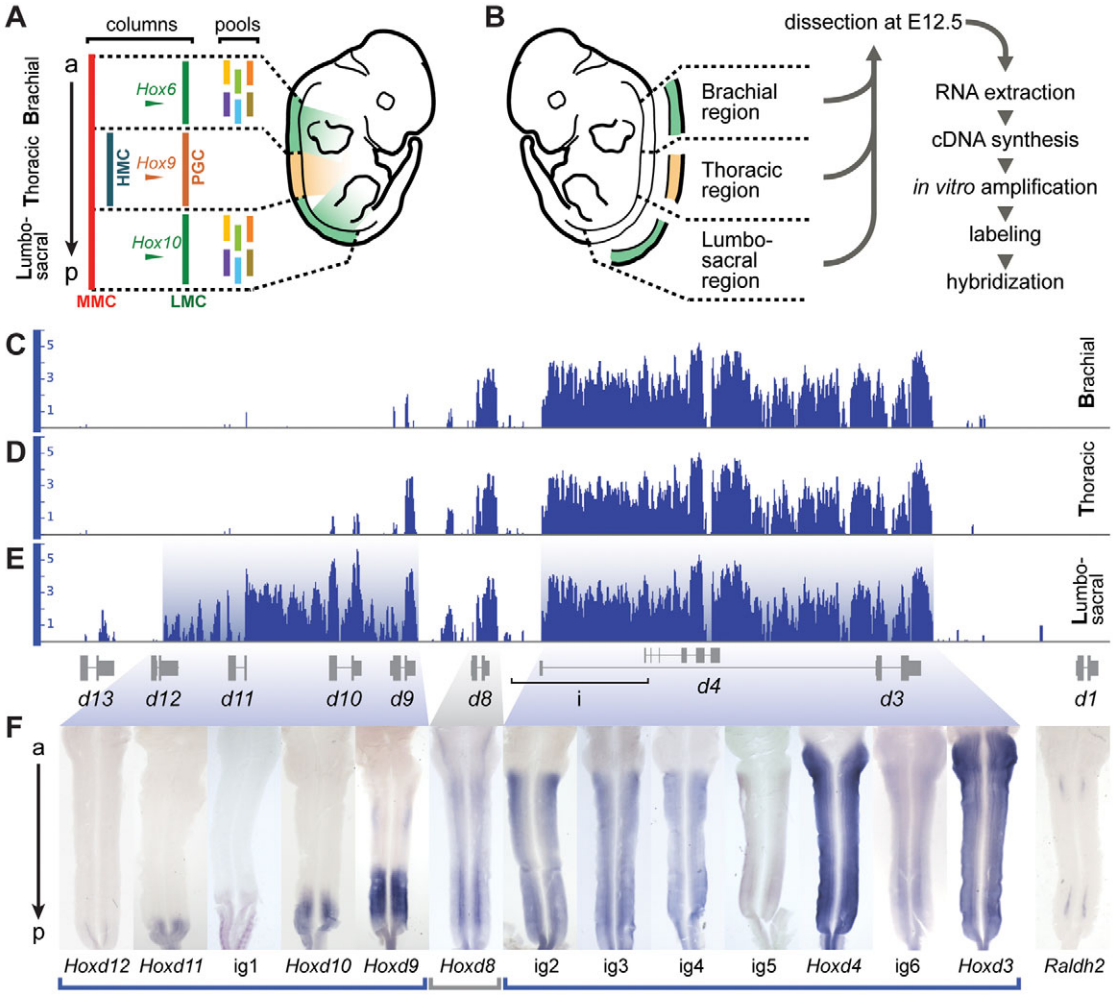


**Fig. 1. Two transcription blocks define the two major rostral boundaries of Hoxd gene expression in the developing spinal cord.** (**A**) Schematic representation of motor neuron organization in the murine spinal cord. Motor neurons are organized along the anterior (a) to posterior (p) axis into discrete columns, namely the MMC, the HMC and the Hox-induced PGC and LMC. The latter is further subdivided into discrete neuronal pools that innervate the limb musculature (see Dasen and Jessell, 2009). (**B**) Flow chart of the experimental approach. Three anatomically defined fragments of E12.5 spinal cords are dissected, RNA extracted, processed and hybridized onto tiling arrays. (**C-E**) Transcription profiles of double-stranded cDNAs at brachial (C), thoracic (D) and lumbosacral levels (E). Annotated exons are shown as grey boxes below, a black bracket demarcates region 'i'. Widespread intergenic transcription defines two transcription blocks, shaded in pale blue, that are separated by stretches of non-transcribed DNA centred on *Hoxd8*, in grey. (**F**) Expression patterns of Hoxd and intergenic (ig) transcripts in open-book spinal cords. Transcripts originating from either the posterior (*Hoxd11* to *Hoxd9*) or the anterior (ig2 to *Hoxd3*) block all show similar rostral boundaries, at either lumbosacral levels or at the brachial plexus/hindbrain, respectively. *Hoxd8* expression displays a transition pattern, including a columnar restricted expression extending up to the midbrain boundary. For better orientation, the positions of the brachial and lumbosacral plexii are indicated by *Raldh2* expression, on the right.

## Two distinct transcription blocks label the two plexii

The transcript distribution at lumbosacral levels seemed to define two separated blocks of transcription. An anterior block covered approximately 40 kb, spanning from region 'i' to the 3′UTR of *Hoxd3*, whereas a ~25 kb large region, extending from *Hoxd12* to *Hoxd9*, also showed widespread transcription in the posterior half of the complex (Fig. 1E, shaded pale blue). Between these two blocks, *Hoxd8* was transcribed at all three anatomical levels. Strikingly, however, *Hoxd8* transcription could not be associated to either the anterior or the posterior block. Instead, this transcription unit showed a clear separation from both blocks, by 5 kb large DNA stretches on either side, devoid of any detectable transcription coming from the Hox-coding strand (Fig. 1E and supplementary material Fig. S1E).

We investigated the expression patterns associated with these two transcription blocks by WISH, in embryos at E12.5 with their spinal cord opened and flat-mounted after staining. We used a battery of probes complementary either to known Hoxd transcription units or to unannotated transcripts, as defined by our tiling array analyses. Again, a clear dichotomy appeared in the expression territories of RNAs derived from the two blocks. Transcripts of the anterior block all had a rostral limit of expression either within, or immediately below the hindbrain (Fig. 1F, right). *Hoxd4* and *Hoxd3* were expressed strongly up into the hindbrain, with the ig6 fragment located in between also being expressed there, though much weaker. Its major transcription boundary, as for all other fragments isolated from this block (ig2 to ig5; Fig. 1F), nicely aligned with the position of the brachial LMCs.

By marked contrast, RNAs derived from the posterior block displayed anterior boundaries within or immediately anterior to the lumbosacral plexus (Fig. 1F, left). *Hoxd8*, however, showed a columnar restricted expression, with signals extending up to mid-brain regions, setting the gene apart from the rest of *HoxD* cluster, in agreement with its isolated transcription profile as seen on tiling arrays. Therefore, rather than displaying a progressively staggered distribution of transcripts along the AP axis, as e.g. in mesoderm derivatives, the collinear boundaries in Hoxd genes transcription are built upon two major territories. They coincide with the functional subdivision of the spinal cord; an anterior block of transcription, labelling the future brachial plexus up into the hindbrain, and a posterior block observed at the level of the lumbosacral plexus.

## Independent regulatory strategies

To gain insight into the regulatory logic underlying these two transcription blocks, we used a series of deletion alleles, produced via the TAMERE approach (Herault et al., 1998b), which remove various parts of the *HoxD* gene cluster. We first challenged the regulatory interdependency of the two apparent blocks of transcriptional activities, by using two deletions removing entirely either one of them; in the Del(1-i) mice, the anterior part of the gene cluster was deleted from *Hoxd1* included to downstream *Hoxd8*, whereas Del(8-13) mice carried a deletion of the posterior half, i.e. from *Hoxd8* included to *Hoxd13* (Fig. 2A-F, shaded grey). E12.5 homozygous mutant spinal cords were isolated, their RNAs extracted and their *HoxD* transcription profiles analyzed.

In the Del(1-i) embryonic spinal cord, weak ectopic signals appeared around the breakpoint, anterior to *Hoxd8* and in the second exon of *Hoxd1*, probably originating from an ectopic transcript spanning the *loxP* site. However, the global transcription profile in the posterior half of the cluster closely followed wild-type patterns all along the spinal cord, indicating that the deletion of the anterior part of the cluster did not substantially alter the transcription in the remaining posterior block (Fig. 2A-C, compare with Fig. 1C-E, left). Likewise, removing the posterior part of the

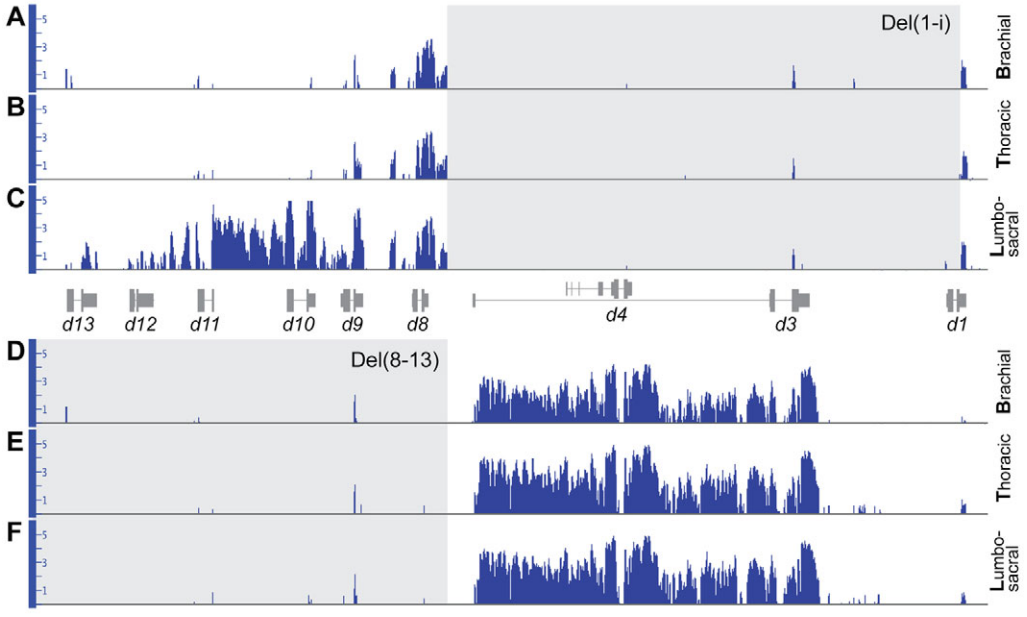


**Fig. 2. Regulatory autonomy of the two *HoxD* transcription blocks.** Tiling array profiles of RNAs extracted from the brachial, thoracic and lumbosacral regions of Del(1-i) homozygote mutant (A-C) and Del(8-13) homozygote mutant (D-F) spinal cords. Grey boxes highlight the extent of the deleted fragments. (**A-C**) Removing the entire anterior transcription block by deleting from *Hoxd1* until region 'i' does not affect the transcriptional output of the posterior block along the three anatomical positions (compare to wild type, Fig. 1C-E, left). (**D-F**) Likewise, eliminating the entire posterior block does not lead to any observable deregulation in the transcription pattern of the anterior block (compare to wild type, Fig. 1C-E, right). The control (wild-type) profiles are those shown in Fig. 1.

*HoxD* complex did not impact upon the transcriptional output of the anterior block, as seen in the Del(8-13) mutant spinal cord, which displayed an 'anterior' profile indistinguishable from the wild-type situation (Fig. 2D-F, compare with Fig. 1C-E, right). We thus concluded that the two transcription blocks are established independently from one another, each one depending on their own regulatory logic and modalities.

## Genetic dissection of regulation

We next investigated the effects of deleting the transcriptionally silent DNA domains around the *Hoxd8* locus, i.e. when the separation between the two blocks was impaired. To this aim, we used a set of deletions removing various central fragments of the gene cluster (Fig. 3B-E, shaded grey), while leaving both the anterior and posterior extremities unmodified. In contrast to the previous series of experiments, we observed important reallocations of transcriptional efficiencies, here visualized at brachial levels. When the broadly transcribed region 'i' was removed, a clear upregulation of *Hoxd8* and *Hoxd9* was scored, as well as increased transcription of the coding exons of *Hoxd3*, whereas intergenic transcripts mapping within the *Hoxd4* to *Hoxd3* region markedly decreased (Fig. 3B, green and red arrows, respectively). Larger deletions moving the *Hoxd10* transcription unit next to either *Hoxd4* or *Hoxd3* led to a strong transcriptional activation of this gene at brachial levels, where it is usually silent (Fig. 3C,D). Although this ectopic activation occurred mostly at the expense of anterior, intergenic transcripts, progressively larger deletions also started to affect the transcriptional output of anterior coding sequences (Fig. 3C-E). Similar reallocations were seen at thoracic and lumbar levels (data not shown). We next investigated the expression patterns associated with these changes using WISH on open-book spinal cords. Consistently, we found transcriptional upregulation of posterior genes located centromeric to the deletion breakpoints along the AP axis of the spinal cord. The resulting ectopic activations along the AP (*Hoxd12*, *Hoxd10*) or dorsoventral (DV) axis (*Hoxd8*) of the spinal cord were mirrored by a decrease in steady-state level transcripts of genes lying telomeric to the breakpoints (*Hoxd4*, *Hoxd3*; Fig. 3F). Therefore, internal deletions abolishing the physical separation of the two transcription blocks led to the ectopic anterior activation of posterior Hoxd genes, at the expense of transcripts belonging to the anterior block (Fig. 3B-F).

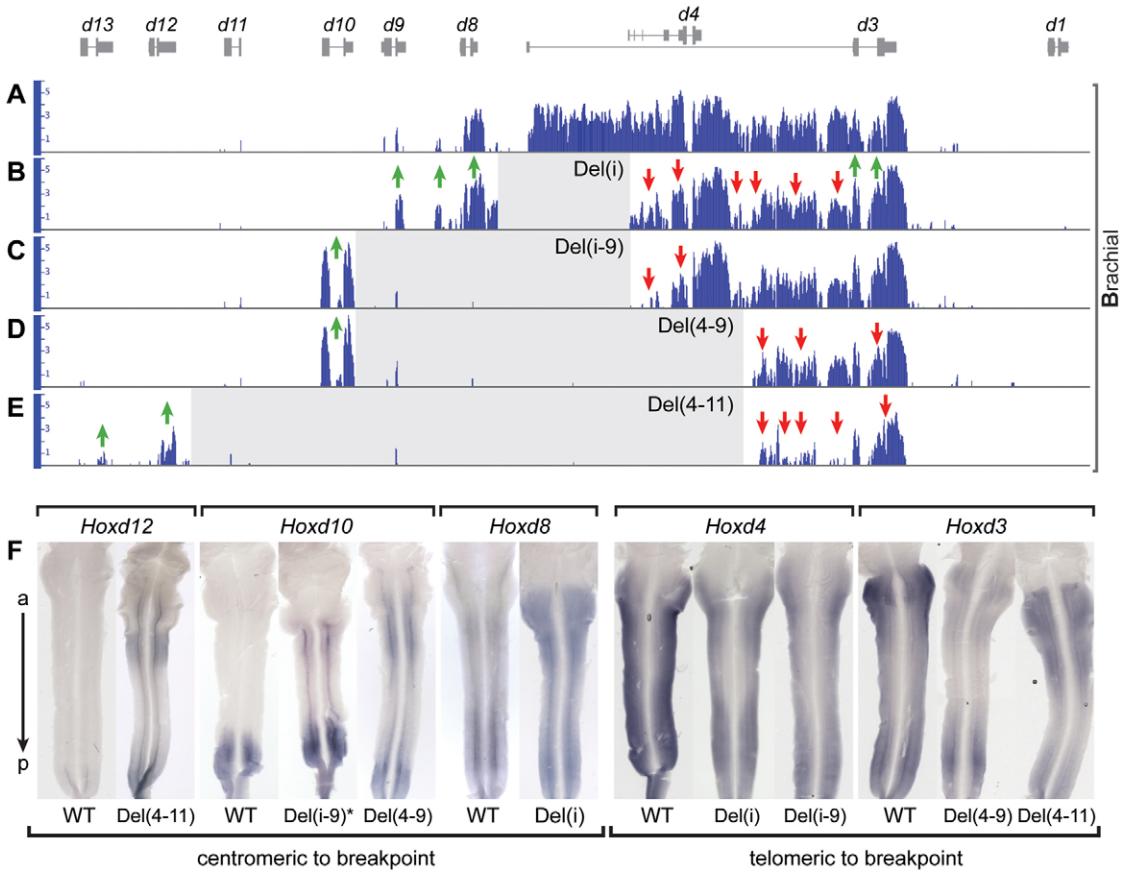


**Fig. 3. Scanning deletion analysis reveals the necessity to properly separate the two *HoxD* transcription blocks.** (**A-E**) Internal deletions (highlighted in grey) that remove the region separating the two blocks lead to ectopic expression of posterior *Hoxd* genes. Tiling array RNA profiles at brachial level, of wild-type control (A), Del(i) (B), Del(i-9) (C), Del(4-9) (D) and Del(4-11) (E) homozygote mutant spinal cords. (B) Deleting region 'i' causes an upregulation of *Hoxd3*, *Hoxd8* and *Hoxd9*, while decreasing the amount of anterior intergenic transcripts (green and red arrows). Larger deletions lead to the ectopic expression of posterior genes at brachial levels, such as for *Hoxd10* in the case of Del(i-9) and Del(4-9) (C,D), or *Hoxd12* in Del(4-11) mutant embryos (E), at the expense of anterior intergenic transcripts and ultimately also of anterior coding regions (C-E). (**F**) Expression patterns of *Hoxd* transcripts in wild-type (WT) and mutant open-book spinal cords. Genes located centromeric to deletion breakpoints are upregulated and expressed ectopically either at anterior levels (*Hoxd12*, *Hoxd10*) or along the DV axis (*Hoxd8*). By contrast, genes located telomeric to the breakpoints largely maintain their expression patterns, although they are transcribed with somewhat lower efficiencies (*Hoxd4*, *Hoxd3*). All mutant spinal cords depicted are homozygote, except Del(i-9), which is heterozygote.

Of the posterior Hoxd genes, *Hoxd10* is instrumental in specifying lumbar LMCs (Carpenter et al., 1997) and its overexpression at anterior levels led to the mis-specification of neuronal fates (Dasen et al., 2003; Shah et al., 2004). Indeed, ectopic transcription of *Hoxd10* in our mutant stocks also resulted in the production of functional protein at anterior levels, as evidenced by HOXD10 immunohistochemistry and the upregulation of its downstream target *FoxP1* (Dasen et al., 2008; Rousso et al., 2008) (supplementary material Fig. S2), thus offering a potential explanation for the apparent necessity to keep the two transcriptional blocks separated, to avoid regulatory interferences leading to neuronal mis-specifications.

## Transgene scanning

These reallocations of local enhancer activities between closely located Hox genes made it difficult to map regulatory sequences in vivo using deletion mutants. We designed a series of contiguous reporter transgenes corresponding exactly to those DNA intervals defined by pairs of *loxP* sites and further deleted by recombination in trans (see Kmita et al., 2002; Tarchini et al., 2005). Seven contiguous transgenes were constructed, covering a total genomic fragment of more than 75 kb from *Hoxd3* to *Hoxd11*, all hooked up in frame to a *lacZ* reporter gene (Fig. 4A and supplementary material Fig. S3). Founder animals were screened for transgene presence, approximate copy number and integrity using PCR- and Southern blot-based genotyping strategies.

F1 animals were crossed to wild-type specimen and E12.5 embryos stained for β-gal activity (Zakany et al., 1988). At least two lines were investigated for each locus, and representative embryos are depicted in Fig. 4B-H. All lines investigated for TgN*d11*lac and TgN*d9*lac showed robust activation in the spinal cord with the expected rostral limits of expression (Fig. 4B,D, arrowheads). TgN*d10*lac lines, by contrast, showed variable results with weak and patchy reporter activity scored in a variety of embryonic structures in the different lines (data not shown). However, none of the lines (0 out of 5) displayed wild-type like activation in the developing spinal cord (Fig. 4C). Likewise, the TgN*d8*lac transgene was completely silent in the spinal cord, the only reproducible activity being found in the developing urogenital system (Fig. 4E; data not shown; 6 out of 7).

In TgN*i*lac animals, the *lacZ* was inserted into an alternative upstream exon of *Hoxd3*. A patchy activity was recovered in the spinal cord, with an anterior limit of expression at approximately the level of the forelimb (Fig. 4F, arrowhead). However, this pattern reflected neither the rostral expression limit, nor the intensity of transcripts originating from the endogenous 'i' locus (compare with Fig. 1F, ig2-4). By contrast, both TgN*d4*lac and TgN*d3*lac showed strong and reproducible staining in the spinal cord. TgN*d4*lac displayed an expression boundary between rhombomeres 6 and 7, as for the endogenous gene, whereas the expression pattern of TgN*d3*lac was slightly anteriorized (Fig. 4G,H, arrowheads). Altogether, this transgene scanning approach revealed that although some of the Hoxd loci display regulatory autonomy in trans, others seem unable to elicit a transcriptional activity by themselves and hence require the context of the cluster in cis to produce their spatially correct gene expression patterns in the spinal cord.

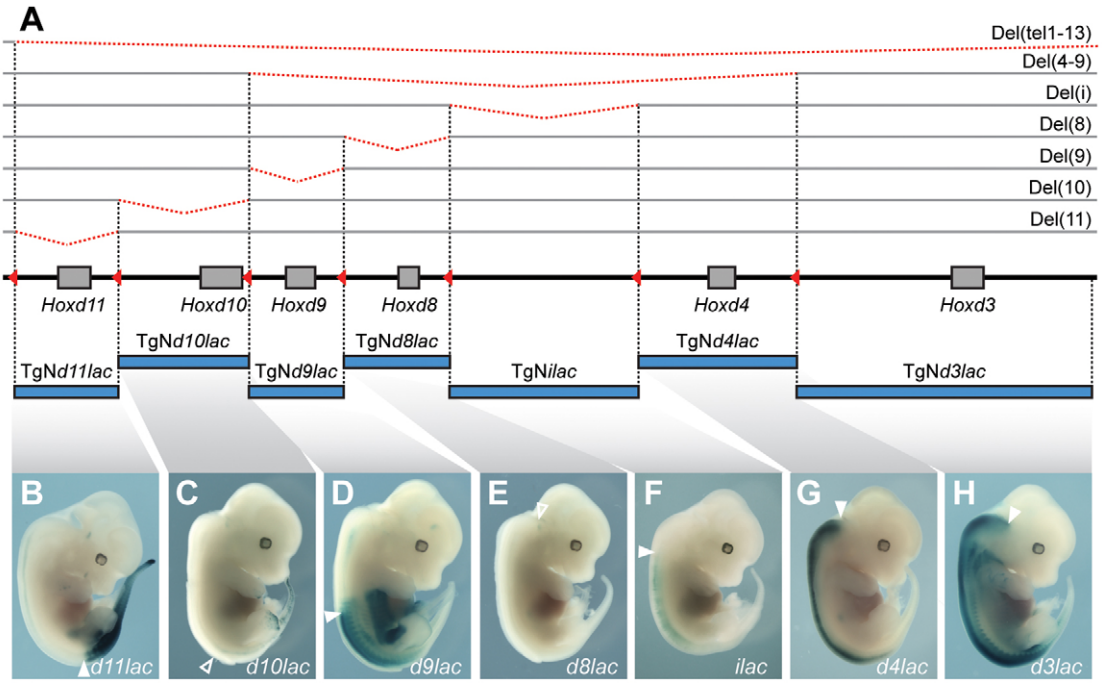


**Fig. 4. A contiguous series of *lacZ* transgenes covering the *HoxD* complex.** (**A**) Schematic map of the murine *HoxD* cluster corresponding to the two major transcription blocks, with genes represented by grey boxes. The positions of *loxP* sites used for the deletions in the complex are shown by red triangles, and red dashed lines above highlight the extent of available balancer deletions used for Fig. 5. (**B-H**) Representative X-gal stained embryos for the different Hoxd transgenic lines at E12.5. Whereas *Hoxd11lac* (B), *Hoxd9lac* (D), *Hoxd4lac* (G) and *Hoxd3lac* (H) show a clear and expected expression in the spinal cord, only trace amounts of β-gal activity is detected for *ilac* (F). No transgene expression in the spinal cord was scored for both *Hoxd10lac* (C) and *Hoxd8lac* (E). Reproducible anterior limits, which were found in at least two transgenic lines, are depicted by solid arrowheads. In their absence, the expected expression limits, as inferred from WISH analyses, are highlighted by empty arrowheads.

### Transcription profiles of Hoxd genes in trans

Although the detection of transgenic β-gal activity reflects the overall regulatory potential of transgenic DNA, it remains poorly informative regarding the exact structure and expression levels of the produced mRNAs. Moreover, transcripts not including the reporter sequence will remain undetected. Because the breakpoints of our deletion stocks correspond exactly to the extremities of our transgenic fragments (Fig. 4A), we investigated their individual RNA profiles on tiling arrays by crossing transgenes over the corresponding deletions. In this way, we reconstituted the *HoxD* gene cluster, yet with one locus at a time in a trans configuration (e.g. *Hoxd9* in Fig. 5A). Accordingly, all transcripts coming from a given endogenous *Hoxd* gene locus are removed (Fig. 5A, grey) and RNAs detected on the tiling array originate exclusively from the transgene (Fig. 5A, orange).

We reduced the transgene copy number to one using *loxP*- or *FRT*-dependent deletions. F1 transgenic animals were crossed to mice harbouring the corresponding gene deletion in the *HoxD* complex. F3 crosses generated E12.5 embryos, which were homozygous for a given deletion, but containing the related transgene. RNA was extracted from the lumbosacral region and processed as before.

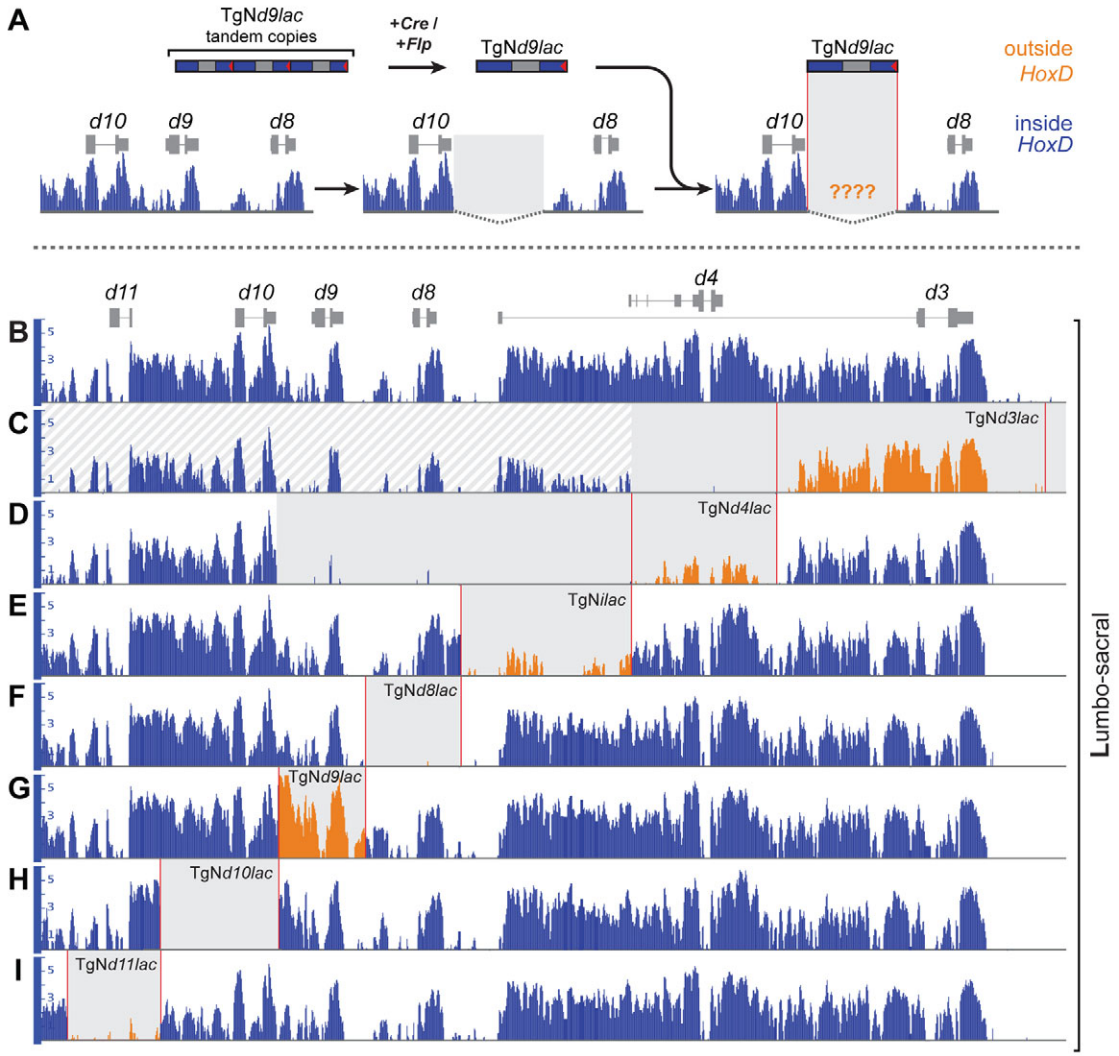


**Fig. 5. Transcription profiles of Hoxd genes in trans.** (**A**) Flow chart of the experimental approach. To investigate the transcription profile of a Hoxd transgene, the corresponding endogenous locus was removed by an appropriate deletion in the cluster. Transgenic animals were crossed to *Cre*- or *Flp*-deleter strains to reduce the transgene copy number to one. The resulting animals are crossed into the respective deletion background and F3 embryos are used for tiling array analyses. (**B-I**) Lumbosacral transcription tiling array profiles of wild-type control (B), TgN*d3lac* (C), TgN*d4lac* (D), TgN*ilac* (E), TgN*d8lac* (F), TgN*d9lac* (G), TgN*d10lac* (H) and TgN*d11lac* (I). Grey boxes highlight the extent of the respective deletions (striped white for heterozygous segments), with the extent of transgenic fragments delineated by red vertical lines. RNA originating from the endogenous *HoxD* locus is shown in blue, RNA coming from the respective Hoxd transgenes is depicted in orange. While the TgN*d3lac* transgene shows an almost wild-type-like expression profile in both peak pattern and intensity (C), both TgN*d4lac* (D) and TgN*ilac* (E) display greatly reduced levels of transcription coming from the transgenic locus. No transgenic RNA is scored for either TgN*d8lac* (E) or TgN*d10lac* (G). Solid transcription is detected across the entire TgN*d9lac* transgene (F). Whereas the pattern on exon 2 and the 3′UTR follows closely the wild-type distribution, ectopic transcripts are scored in the 5′ region of the transgene. Only small peaks corresponding to the highest wild-type signals are detected for TgN*d11lac* (H). Genotypes are as follows: wild-type control (B), Del(1-4)/Del(tel1-13)*d11*lac; TgN*d3lac*$^{+}$ (C), Del(4-9)$^{-/-}$; TgN*d4lac*$^{+}$ (D), Del(i)$^{-/-}$; TgN*ilac*$^{+}$ (E), Del(8)$^{-/-}$; TgN*d8lac*$^{+}$ (F), Del(9)$^{-/-}$; TgN*d9lac*$^{+}$ (G), Del(10)$^{-/-}$; TgN*d10lac*$^{+}$ (H), and Del(11)$^{-/-}$; TgN*d11lac*$^{+}$ (I).

In agreement with their lack of *lacZ* expression in the spinal cord, neither the TgN*d8*lac, nor the TgN*d10*lac transgenes showed any RNA signal (Fig. 5F,H). By contrast, the TgN*d9*lac construct, which showed a strong and rather faithful distribution of β-gal activity in transgenic embryos, displayed widespread and solid transcription throughout the locus in trans (Fig. 5G). Whereas the second coding exon of the transgene showed an RNA profile close to the endogenous gene, increased transcription levels were apparent at the 5′ end of the transgenic profile. The expression profile of the TgN*d11*lac transgene, on the other hand, displayed only weak peaks, at those locations where the strongest signals were observed in the endogenous locus. This discrepancy between the two transgenes showing apparently comparable amounts of β-gal activity can be explained both by a dilution effect, as only the posterior segment of the dissected lumbosacral piece stained positive for the TgN*d11*lac transgene, and by the biochemical properties of the X-gal staining (see Discussion).

When selected from within the anterior block of transcription, all transgenes showed *lacZ* staining and RNA signals on the tiling array, albeit with greatly varying intensities. A cluster of small peaks originating from the alternative *Hoxd3* promoter where our reporter gene was integrated reflected the weak β-gal activity seen in TgN*i*lac embryos (Fig. 5E). Likewise, the TgN*d4*lac profile globally matched the output of the endogenous locus, but again at greatly reduced levels (Fig. 5D). TgN*d3*lac, however, looked nearly indistinguishable from the endogenous profile (Fig. 5C).

This systematic analysis of TgN*Hox*lac in spinal cords thus uncovered important differences in the transcriptional efficiencies of the various gene loci. Whereas some loci (e.g. *Hoxd9*, *Hoxd3*) could efficiently reproduce their endogenous transcription patterns in trans, other loci remained completely silent (*Hoxd8*, *Hoxd10*). This suggested that their normal expression, as observed in wild-type animals, is controlled by regulatory elements located within the neighbouring loci.

## DISCUSSION

The functional importance of Hox proteins in patterning the spinal cord along its AP axis, in particular in the determination of neuronal identities, has been well established (Dasen and Jessell, 2009). Yet, the mechanisms generating the necessary expression patterns, at the transcriptional level, are far less well documented. In many animal species, important aspects of the spatial Hox transcripts distribution are intrinsically linked to the clustered organization of these genes, a phenomenon known as spatial collinearity (Kmita and Duboule, 2003). Paradoxically, however, while the relative position of a gene within the cluster correlates with its rostral limits of expression, the presence of an intact cluster does not seem to be a strict prerequisite for this phenomenon to occur. For example, rather faithful expression patterns were observed for a number of randomly integrated Hox transgenes in the mouse (e.g. Puschel et al., 1991; Gerard et al., 1993). Also, the endogenous Hox genes in the larvacean *Oikopleura* are expressed with some collinear features, even though a gene cluster does not exist in this species (Seo et al., 2004). This may reflect the fact that an important part of the regulatory machinery necessary to define the spatial distribution of transcripts often resides in close proximity to the target genes, interspersed inside the Hox clusters (Whiting et al., 1991; Tschopp et al., 2009).

However, the results presented here suggest that the correct establishment of spatial collinearity in the mouse spinal cord also relies heavily upon the presence of a gene cluster at least partially organized. We find that extended stretches of the *HoxD* cluster are actively transcribed from multiple promoters, playing an important role in fine-tuning the overall transcriptional outcome of the different gene loci. In particular, we report the presence of two distinct transcription blocks, inside the *HoxD* gene cluster, that define two general expression territories. The first block involves mostly the transcription of both *Hoxd3* and *Hoxd4* all along the spinal cord, including both future plexii. The second block involves more posterior genes (from *Hoxd9* to *Hoxd11*) and is restricted to a caudal part of the spinal cord, containing the future lumbosacral plexus. Therefore, these distinct regulatory modalities generate different genetic addresses at the level of the future plexii, which will subsequently innervate the musculature of tetrapod limbs. Within the two blocks, sharing of ‘enhancer mini-hubs’ may be required for efficient Hoxd transcription, a fact that establishes an inter-dependency between neighbouring gene loci and provides an additional layer of constraint to keep vertebrate Hox genes tightly clustered.

### Two virtual *HoxD* subclusters

The presence of two distinct transcription blocks somewhat echoes the situation found in various dipteran species, where the ancestral Hox complex is split into two independent genomic subclusters (Duboule and Dolle, 1989; Graham et al., 1989). Although transcriptional regulation inside the two *HoxD* blocks relies upon shared enhancer elements, these two regulatory domains appear functionally independent from one another, defining two virtual subclusters (see Fig. 3A-F). Indeed, in the case of the spinal cord, the observed regulatory autonomy would probably allow for a *Diptera*-like split of the murine *HoxD* complex at or around the position of *Hoxd8*, thus separating ‘posterior’ genes (i.e. those related to *Abdominal-B*) strongly expressed in the lumbosacral plexus, from anterior Hox genes, heavily transcribed at both lumbar and brachial levels. Regulatory constraints imposed in other tissues, however, will prevent such a split from occurring (e.g. Tarchini and Duboule, 2006; Tschopp et al., 2009).

Each one of these two transcription blocks contains one locus that can elicit very strong expression in a transgenic context. In the anterior spinal cord, TgN*d3*lac clearly included a strong enhancer activity, whereas TgN*d9*lac was its counterpart in the posterior spine. Some loci located nearby (*Hoxd4* and *Hoxd11*) were also able to drive transcription within the spinal cord, although with a substantially lower efficiency, an observation that was probably overlooked when contemplating previous X-gal stainings (Gerard et al., 1993; Zhang et al., 1997). We think this is because of a saturation effect, the stability of the β-gal protein and multicopy insertions in the conditions initially analyzed. Nevertheless, weak but clear signals were scored from both the *Hoxd4* and *Hoxd11* loci, suggesting that although these promoters can indeed respond to local enhancers elements, their full activities somehow rely on the heavy transcriptional activity of either the *Hoxd3*, or the *Hoxd9* loci in cis. This is supported by previous observations reporting the impact of the *Hoxd9* locus on the transcription of both *Hoxd10* and *Hoxd11* (Tarchini et al., 2005). In this view, the *Hoxd3* and *Hoxd9* loci may organize local ‘enhancer mini-hubs’ (Fig. 6, green halos), a situation that would explain the need for clustering within each of these blocks, to set up spatial collinearity at the proper quantitative levels. Once controlled by these mini-hubs, local and gene-specific regulatory elements may account for the slight expression differences observed within each of the two transcription blocks, along the AP and DV axes for the different Hoxd genes (see e.g. Fig. 1F).

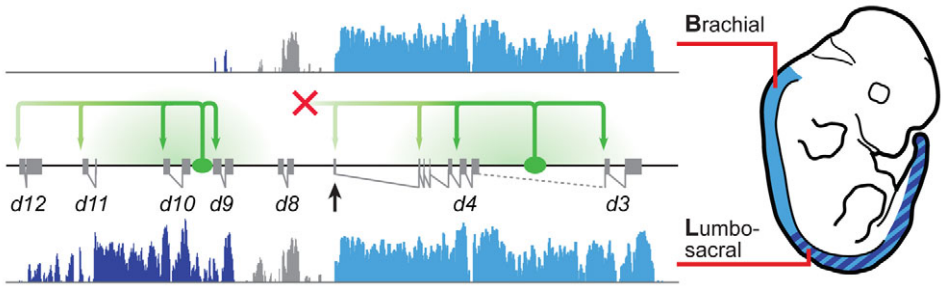


**Fig. 6. Two transcription blocks set up the spatial collinear expression of Hoxd gene in the spinal cord.** Two major rostral boundaries are present for Hoxd genes, which coincide with the functional subdivision of the spinal cord at the level of the hindbrain and brachial plexus anteriorly, and the lumbosacral plexus posteriorly. At the transcriptional level, these expression limits manifest themselves as two distinct anterior and posterior blocks (light and dark blue, respectively), separated by silent domains centred on *Hoxd8* (grey), thereby defining two *HoxD* regulatory subclusters. Inside these blocks, local 'enhancer mini-hubs' (green halos) drive the required gene activities, shared between neighbouring genes, whereas promoter competition for anterior enhancers titrates their activities to prevent ectopic expression of posterior Hoxd genes (right, red cross).

## Promoter competition and enhancer titration

Hox clusters display very dense transcriptional activities, owing to the presence of numerous alternative transcription start sites and enhancers intermingled within the coding regions (Mainguy et al., 2007; Rinn et al., 2007; Coulombe et al., 2010). Accordingly, we find extensive transcription outside the annotated coding sequences of the *HoxD* complex, which contribute to delineate the two distinct transcription blocks. When considering single-gene and larger deletions, an intricate regulatory interdependency of these transcripts and the various coding sequences is emerging.

Whereas the deletion of the *Hoxd9* locus decreases the relative amounts of *Hoxd10* coding transcripts (Fig. 5B,G, compare *Hoxd10* with *Hoxd11*), removing this putative enhancer titration effect of *Hoxd10* increases transcription in the 5′ region of *Hoxd9* in Del(10) mutant spinal cords (Fig. 5H). A similar upregulation is seen for the TgN*d9*lac transgene, i.e. when the titrating influence *Hoxd10* is equally removed (Fig. 5G). Moreover, perturbing this subtle transcriptional balance also leads to important changes in the spatial patterns of the genes involved (Tarchini et al., 2005), a consequence difficult to document when considering the entire lumbosacral region as in our tiling array approach.

Transgenic analyses have revealed a complex enhancer landscape within the relatively short *HoxD* genomic interval (Fig. 4) (Renucci et al., 1992; Gerard et al., 1993; Zhang et al., 1997; Herault et al., 1998a). Regulatory elements may act rather generically on any of the surrounding promoters, a situation illustrated by genes lacking the required enhancer elements in their vicinity that hijack the proper controls from their neighbours (e.g. Fig. 4C) (Gould et al., 1997). In this view, the presence of numerous intergenic transcripts within region 'i', i.e. starting from promoters located downstream of *Hoxd8* (Fig. 6, arrow) may simply reflect the necessity to titrate such activities coming from the *Hoxd3* 'enhancer mini-hub'. These promoters would compete for 'anterior' enhancers and thereby prevent the same regulatory influence to reach the more posterior and potentially deleterious genes (Fig. 6, red cross). When aligning these DNA sequences to the three other murine Hox clusters, putative promoters sequences located around group 6 Hox genes score the highest (data not shown). The *HoxD* cluster has lost its group 6 gene at an early stage during gnathostome evolution (Ravi et al., 2009) and it is conceivable that some of its associated promoter elements were maintained there simply owing to their crucial role in the trapping of an anterior regulatory influence.

## A bimodal regulation for two anatomical levels

The appearance of paired appendages was a major innovation in early vertebrates, crucial for their successful radiation. It is believed that the molecular mechanisms underlying the development of paired fins were co-opted from median fins. This structure, which is already observed in agnathans, was not restricted to any particular AP level (Freitas et al., 2006). Therefore, the emergence of paired appendages required the concomitant development of localized and highly specialized nervous plexii, to provide the innervation for their increasingly complex target musculature. In tetrapods, the interpretation of specific combinations of Hox proteins by their target genes underlies this diversification of motor neuron pools at brachial and lumbosacral levels (Dasen et al., 2005; Dasen et al., 2008; Rousso et al., 2008).

The regulatory split of the *HoxD* gene cluster described in this study may give a hint as to how such differential Hox combinations were achieved at the transcriptional level, by evolving distinct and independent regulatory modules based on, and constrained by, the collinear properties of Hox gene clusters. Firstly, the two separate transcription blocks define two major rostral boundaries in the spinal cord, with Hoxd genes either expressed up to brachial and hindbrain regions or confined within lumbosacral limits. Secondly, inside the two blocks, additional enhancer elements further subdivide and fine-tune the major regulatory input from the two 'enhancer mini-hubs' to eventually elicit slightly differential expression patterns, thereby diversifying combinations of Hox proteins.

Alternatively, only few Hox proteins, rather than combinations, may be decisive for motor neuron specification in both plexii, a possibility difficult to demonstrate owing to the redundancy and complementarity of the system, under physiological conditions. An extreme view of this latter possibility would consider the intricate transcription profiles described in this work as being merely the by-products of a general regulatory strategy to ensure that one particular protein be present in neuronal precursors, at the right time and place. Anterior Hoxd proteins do not seem to exert a strong function in the brachial plexus, unlike HOXD10 at the lumbosacral level. *Hoxd3* with its strong anterior enhancers, however, is required for the patterning of the cervical nerves (Condie and Capecchi, 1993). The observed bimodal control of the *HoxD* cluster in the spinal cord may thus have been selected primarily to prevent the deleterious gain-of-function effects of posterior proteins, while at the same time ensuring the appropriate expression levels of the decisive Hoxd products at the correct AP level.

**Acknowledgements**
We thank S. Arber, J. Dasen and C. Tabin for critical comments and suggestions, as well as for the generous gifts of antibodies. We also thank N. Fraudeau for technical assistance, S. Falk and L. Sommer for help with IHC protocols, C. Barraclough and P. Descombes for help with tiling arrays, B. Mascrez for mouse lines as well as members of the Duboule laboratories for discussions and reagents.

**Funding**
This work was supported by funds from the University of Geneva; the Ecole Polytechnique Fédérale, Lausanne; the Swiss National Research Fund; the National Research Center (NCCR) Frontiers in Genetics; and the ERC grant SystemsHox.ch.

**Competing interests statement**
The authors declare no competing financial interests.

**Author contributions**
P.T. and D.D. designed the experiments. P.T. carried out all experiments and was helped by A.J.C. P.T. and D.D. wrote the paper.

**Supplementary material**
Supplementary material available online at
http://dev.biologists.org/lookup/suppl/doi:10.1242/dev.076794/-/DC1

**References**

**Bel-Vialar, S., Itasaki, N. and Krumlauf, R.** (2002). Initiating Hox gene expression: in the early chick neural tube differential sensitivity to FGF and RA signaling subdivides the HoxB genes in two distinct groups. *Development* **129**, 5103-5115.

**Carpenter, E. M., Goddard, J. M., Davis, A. P., Nguyen, T. P. and Capecchi, M. R.** (1997). Targeted disruption of Hoxd-10 affects mouse hindlimb development. *Development* **124**, 4505-4514.

**Condie, B. G. and Capecchi, M. R.** (1993). Mice homozygous for a targeted disruption of Hoxd-3 (Hox-4.1) exhibit anterior transformations of the first and second cervical vertebrae, the atlas and the axis. *Development* **119**, 579-595.

**Coulombe, Y., Lemieux, M., Moreau, J., Aubin, J., Joksimovic, M., Berube-Simard, F. A., Tabaries, S., Boucherat, O., Guillou, F., Larochelle, C. et al.** (2010). Multiple promoters and alternative splicing: Hoxa5 transcriptional complexity in the mouse embryo. *PLoS ONE* **5**, e10600.

**Dasen, J. S. and Jessell, T. M.** (2009). Hox networks and the origins of motor neuron diversity. *Curr. Top. Dev. Biol.* **88**, 169-200.

**Dasen, J. S., Liu, J. P. and Jessell, T. M.** (2003). Motor neuron columnar fate imposed by sequential phases of Hox-c activity. *Nature* **425**, 926-933.

**Dasen, J. S., Tice, B. C., Brenner-Morton, S. and Jessell, T. M.** (2005). A Hox regulatory network establishes motor neuron pool identity and target-muscle connectivity. *Cell* **123**, 477-491.

**Dasen, J. S., De Camilli, A., Wang, B., Tucker, P. W. and Jessell, T. M.** (2008). Hox repertoires for motor neuron diversity and connectivity gated by a single accessory factor, FoxP1. *Cell* **134**, 304-316.

**Duboule, D. and Dolle, P.** (1989). The structural and functional organization of the murine HOX gene family resembles that of Drosophila homeotic genes. *EMBO J.* **8**, 1497-1505.

**Featherstone, M. S., Baron, A., Gaunt, S. J., Mattei, M. G. and Duboule, D.** (1988). Hox-5.1 defines a homeobox-containing gene locus on mouse chromosome 2. *Proc. Natl. Acad. Sci. USA* **85**, 4760-4764.

**Fetcho, J. R.** (1992). The spinal motor system in early vertebrates and some of its evolutionary changes. *Brain Behav. Evol.* **40**, 82-97.

**Freitas, R., Zhang, G. and Cohn, M. J.** (2006). Evidence that mechanisms of fin development evolved in the midline of early vertebrates. *Nature* **442**, 1033-1037.

**Gerard, M., Duboule, D. and Zakany, J.** (1993). Structure and activity of regulatory elements involved in the activation of the Hoxd-11 gene during late gastrulation. *EMBO J.* **12**, 3539-3550.

**Gerard, M., Chen, J. Y., Gronemeyer, H., Chambon, P., Duboule, D. and Zakany, J.** (1996). In vivo targeted mutagenesis of a regulatory element required for positioning the Hoxd-11 and Hoxd-10 expression boundaries. *Genes Dev.* **10**, 2326-2334.

**Gould, A., Morrison, A., Sproat, G., White, R. A. and Krumlauf, R.** (1997). Positive cross-regulation and enhancer sharing: two mechanisms for specifying overlapping Hox expression patterns. *Genes Dev.* **11**, 900-913.

**Graham, A., Papalopulu, N. and Krumlauf, R.** (1989). The murine and Drosophila homeobox gene complexes have common features of organization and expression. *Cell* **57**, 367-378.

**Gutman, C. R., Ajmera, M. K. and Hollyday, M.** (1993). Organization of motor pools supplying axial muscles in the chicken. *Brain Res.* **609**, 129-136.

**Herault, Y., Beckers, J., Kondo, T., Fraudeau, N. and Duboule, D.** (1998a). Genetic analysis of a Hoxd-12 regulatory element reveals global versus local modes of controls in the HoxD complex. *Development* **125**, 1669-1677.

**Herault, Y., Rassoulzadegan, M., Cuzin, F. and Duboule, D.** (1998b). Engineering chromosomes in mice through targeted meiotic recombination (TAMERE). *Nat. Genet.* **20**, 381-384.

**Hollyday, M.** (1980). Motoneuron histogenesis and the development of limb innervation. *Curr. Top. Dev. Biol.* **15**, 181-215.

**Izpisua-Belmonte, J. C., Dolle, P., Renucci, A., Zappavigna, V., Falkenstein, H. and Duboule, D.** (1990). Primary structure and embryonic expression pattern of the mouse Hox-4.3 homeobox gene. *Development* **110**, 733-745.

**Izpisua-Belmonte, J. C., Falkenstein, H., Dolle, P., Renucci, A. and Duboule, D.** (1991). Murine genes related to the Drosophila AbdB homeotic genes are sequentially expressed during development of the posterior part of the body. *EMBO J.* **10**, 2279-2289.

**Jung, H., Lacombe, J., Mazzoni, E. O., Liem, K. F., Jr, Grinstein, J., Mahony, S., Mukhopadhyay, D., Gifford, D. K., Young, R. A., Anderson, K. V. et al.** (2010). Global control of motor neuron topography mediated by the repressive actions of a single hox gene. *Neuron* **67**, 781-796.

**Kmita, M. and Duboule, D.** (2003). Organizing axes in time and space; 25 years of colinear tinkering. *Science* **301**, 331-333.

**Kmita, M., Fraudeau, N., Herault, Y. and Duboule, D.** (2002). Serial deletions and duplications suggest a mechanism for the collinearity of Hoxd genes in limbs. *Nature* **420**, 145-150.

**Landmesser, L.** (1978). The development of motor projection patterns in the chick hind limb. *J. Physiol.* **284**, 391-414.

**Landmesser, L. T.** (2001). The acquisition of motoneuron subtype identity and motor circuit formation. *Int. J. Dev. Neurosci.* **19**, 175-182.

**Liu, J. P., Laufer, E. and Jessell, T. M.** (2001). Assigning the positional identity of spinal motor neurons: rostrocaudal patterning of Hox-c expression by FGFs, Gdf11, and retinoids. *Neuron* **32**, 997-1012.

**Ma, L. H., Gilland, E., Bass, A. H. and Baker, R.** (2010). Ancestry of motor innervation to pectoral fin and forelimb. *Nat. Commun.* **1**, 1-8.

**Mainguy, G., Koster, J., Woltering, J., Jansen, H. and Durston, A.** (2007). Extensive polycistronism and antisense transcription in the mammalian Hox clusters. *PLoS ONE* **2**, e356.

**Nordstrom, U., Maier, E., Jessell, T. M. and Edlund, T.** (2006). An early role for WNT signaling in specifying neural patterns of Cdx and Hox gene expression and motor neuron subtype identity. *PLoS Biol.* **4**, e252.

**Puschel, A. W., Balling, R. and Gruss, P.** (1991). Separate elements cause lineage restriction and specify boundaries of Hox-1.1 expression. *Development* **112**, 279-287.

**Ravi, V., Lam, K., Tay, B. H., Tay, A., Brenner, S. and Venkatesh, B.** (2009). Elephant shark (*Callorhinchus milii*) provides insights into the evolution of Hox gene clusters in gnathostomes. *Proc. Natl. Acad. Sci. USA* **106**, 16327-16332.

**Renucci, A., Zappavigna, V., Zakany, J., Izpisua-Belmonte, J. C., Burki, K. and Duboule, D.** (1992). Comparison of mouse and human HOX-4 complexes defines conserved sequences involved in the regulation of Hox-4.4. *EMBO J.* **11**, 1459-1468.

**Rinn, J. L., Kertesz, M., Wang, J. K., Squazzo, S. L., Xu, X., Brugmann, S. A., Goodnough, L. H., Helms, J. A., Farnham, P. J., Segal, E. et al.** (2007). Functional demarcation of active and silent chromatin domains in human HOX loci by noncoding RNAs. *Cell* **129**, 1311-1323.

**Rousso, D. L., Gaber, Z. B., Wellik, D., Morrisey, E. E. and Novitch, B. G.** (2008). Coordinated actions of the forkhead protein Foxp1 and Hox proteins in the columnar organization of spinal motor neurons. *Neuron* **59**, 226-240.

**Seo, H. C., Edvardsen, R. B., Maeland, A. D., Bjordal, M., Jensen, M. F., Hansen, A., Flaat, M., Weissenbach, J., Lehrach, H., Wincker, P. et al.** (2004). *Hox* cluster disintegration with persistent anteroposterior order of expression in *Oikopleura dioica*. *Nature* **431**, 67-71.

**Shah, V., Drill, E. and Lance-Jones, C.** (2004). Ectopic expression of Hoxd10 in thoracic spinal segments induces motoneurons with a lumbosacral molecular profile and axon projections to the limb. *Dev. Dyn.* **231**, 43-56.

**Sharpe, J., Nonchev, S., Gould, A., Whiting, J. and Krumlauf, R.** (1998). Selectivity, sharing and competitive interactions in the regulation of Hoxb genes. *EMBO J.* **17**, 1788-1798.

**Soshnikova, N. and Duboule, D.** (2009). Epigenetic temporal control of mouse Hox genes in vivo. *Science* **324**, 1320-1323.

**Tarchini, B. and Duboule, D.** (2006). Control of Hoxd genes' collinearity during early limb development. *Dev. Cell* **10**, 93-103.

**Tarchini, B., Huynh, T. H., Cox, G. A. and Duboule, D.** (2005). HoxD cluster scanning deletions identify multiple defects leading to paralysis in the mouse mutant Ironside. *Genes Dev.* **19**, 2862-2876.

**Tschopp, P., Tarchini, B., Spitz, F., Zakany, J. and Duboule, D.** (2009). Uncoupling time and space in the collinear regulation of Hox genes. *PLoS Genet.* **5**, e1000398.

**Wahba, G. M., Hostikka, S. L. and Carpenter, E. M.** (2001). The paralogous Hox genes Hoxa10 and Hoxd10 interact to pattern the mouse hindlimb peripheral nervous system and skeleton. *Dev. Biol.* **231**, 87-102.

**Whiting, J., Marshall, H., Cook, M., Krumlauf, R., Rigby, P. W., Stott, D. and Allemann, R. K.** (1991). Multiple spatially specific enhancers are required to reconstruct the pattern of Hox-2.6 gene expression. *Genes Dev.* **5**, 2048-2059.

**Yu, D., Ellis, H. M., Lee, E. C., Jenkins, N. A., Copeland, N. G. and Court, D. L.** (2000). An efficient recombination system for chromosome engineering in Escherichia coli. *Proc. Natl. Acad. Sci. USA* **97**, 5978-5983.

**Zacchetti, G., Duboule, D. and Zakany, J.** (2007). Hox gene function in vertebrate gut morphogenesis: the case of the caecum. *Development* **134**, 3967-3973.

**Zakany, J., Tuggle, C. K., Patel, M. D. and Nguyen-Huu, M. C.** (1988). Spatial regulation of homeobox gene fusions in the embryonic central nervous system of transgenic mice. *Neuron* **1**, 679-691.

**Zappavigna, V., Renucci, A., Izpisua-Belmonte, J. C., Urier, G., Peschle, C. and Duboule, D.** (1991). HOX4 genes encode transcription factors with potential auto- and cross-regulatory capacities. *EMBO J.* **10**, 4177-4187.

**Zhang, F., Popperl, H., Morrison, A., Kovacs, E. N., Prideaux, V., Schwarz, L., Krumlauf, R., Rossant, J. and Featherstone, M. S.** (1997). Elements both 5′ and 3′ to the murine Hoxd4 gene establish anterior borders of expression in mesoderm and neurectoderm. *Mech. Dev.* **67**, 49-58.